

Electronic Supporting Information

Insights on the Cold Plasma Ammonia Synthesis and Decomposition using alkaline earth metal-based Perovskites

*Fnu Gorky,^a Jolie M. Lucero,^b James M. Crawford,^b Beth A. Blake,^a Shelby R. Guthrie,^a Moises A. Carreon,^b and Maria L. Carreon^{*a}*

^aChemical and Biological Engineering Department, South Dakota School of Mines & Technology, 501 E Saint Joseph St, Rapid City, South Dakota– 57701, USA

^bChemical and Biological Engineering Department, Colorado School of Mines, Golden, CO 8040, USA

*Corresponding author: Maria.CarreonGarciduenas@sdsmt.edu

Table of Contents

S1. State of The Art.....	S2
S2. Average crystal size of perovskite catalysts.....	S3
S3. OES Plasma Only Vs. MgTiO ₃	S4
S4. Repeating Cycles for MgTiO ₃	S5
S5. Spent Perovskite (FTIR Spectra).....	S6
S6. OES for MgTiO ₃ at different plasma Power (5W, 10W, 20 W).....	S7
S7. Equations employed.....	S8
S8. Only Plasma (N ₂ :H ₂) Vs Helium Dilution (N ₂ :H ₂ :He).....	S9
S9. OES for MgTiO ₃ with & without Helium Dilution at Constant Watts.....	S10
S10. OES for NH ₃ Decomposition for MgTiO ₃ at different Watts.....	S11
S11. Comparison on perovskites performance (State-of-the-Art)	S12
S12. Reactor Electrical Characterization.....	S13
S13. Details on Mechanism Plot (Figure 8)	S14
S14. Details on Ammonia Calibration Curve.....	S15
S15. Live Gas Chromatography report for identification of ammonia peak.....	S16
S16. DBD Reactor Setup.....	S17
S17. Surface area (m ² g ⁻¹) of the perovskite samples.....	S18
S18. Perovskites Porosity (ϕ) (Fresh Vs. Spent)	S19
S19. References	S20

State of The Art

Table S1 Summary of the literature on ammonia production over Mg based catalysts.

Year	Catalysis ^I	Catalyst	Flow Rate	Pressure	H ₂ /N ₂ Ratio	Voltage	NH ₃ Yield	NH ₃ Synthesis Rate ^{II}	Energy Yield	TOF	Reference		
			$\frac{ml}{min}$	Bar	-	kV	%	$\frac{\mu mol}{min \cdot gcat}$	$\frac{g \text{ of } NH_3}{kW.h}$	s^{-1}			
1986	NTP-DBD	MgO	160	1	3	-	3.1	-	-	-	2		
1992	Thermal	Ru/MgO	60	0.8	3	-	-	3	-	1.8×10^{-4}	3		
2000	NTP-DBD	MgO	2266.7	0.006	0.8	0.5	0.3	-	-	-	4		
2001	Thermal	Ba-Ru/MgO	40	1	3	-	-	31.9	-	26.9×10^{-4}	5		
2002	Thermal	Cs-Ru/MgO	40	63	3	-	-	32	-	27×10^{-4}	6		
2016	NTP-DBD	Cs-Ru/MgO	4000	1	3	6	2.4	-	2.3	-	7		
2016	NTP-DBD	Ru-Mg/Al ₂ O ₃	2000	1	0.25	5.4	2.5	-	35.7	-	8		
2019	NTP-DBD	MgCl ₂	4000	1	1	6.4	-	50	20.5	-	9		
2020	NTP-DBD	MgO	400	1	3	17	0.2	-	20.5	-	10		
2020	Thermal	Ba+Co/Mg-La	1167	90	3	-	11	-	-	-	11		
2021	NTP-DBD	This study (MgTiO ₃)	25	1	1	16	0.5	73.4	3.7	-	-		
			25	1	1	8	0.3	36.1	7.3	-	-		
Catalysis^I NTP-DBD (Non-Thermal Plasma Dielectric Barrier Discharge) & Thermal Catalysis													
NH₃ Synthesis Rate^{II} We are presenting the units with $\mu mol \text{ min}^{-1} \text{ gcat}^{-1}$ in order to homogenize with the present literature.													

Catalyst Characterization (Average Crystal Size)

Perovskite	Fresh(μm)	Spent(μm)
MgTiO₃	2.50±0.90	2.20±0.80
SrTiO₃	1.40±0.70	1.50±0.80
CaTiO₃	1.00±0.70	1.40±0.70
BaTiO₃	0.80±0.40	0.90±0.50

Table S2 Average crystal size of all studied perovskite catalysts: fresh and spent.

OES for Plasma Only Vs. MgTiO₃

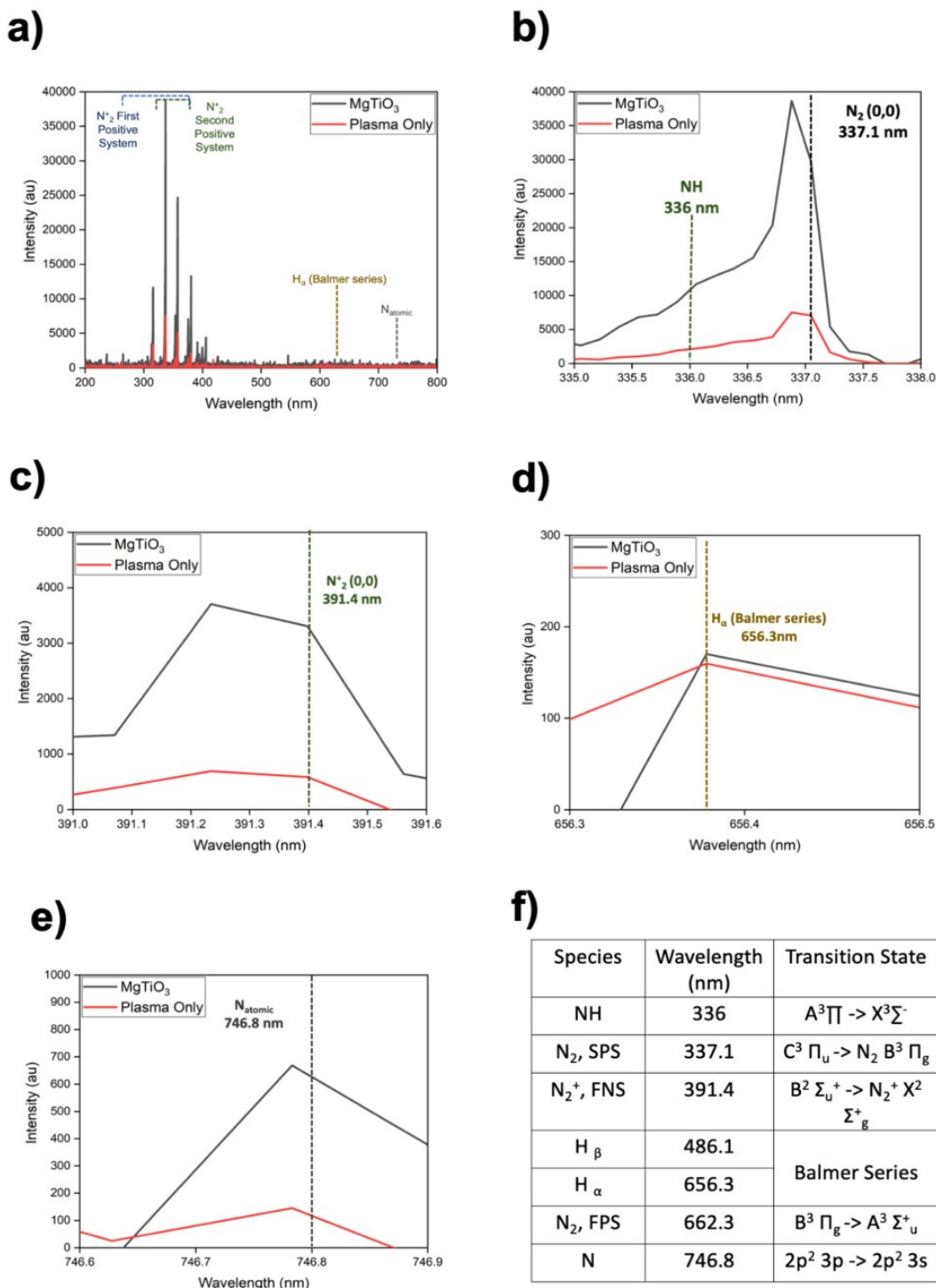


Figure S1 Emission spectra collected during plasma catalytic ammonia synthesis: (a), (b), (c), (d) Emission spectrum of N₂, NH, N₂⁺, H_α, and N_{atomic} at 1:1 N₂:H₂ feed ratio MgTiO₃ Vs Plasma Only feed ratio MgTiO₃ at Power (Watts) (20 W) (average bulk temperature of 210 °C) and f) summary of important plasma species.

Repeating Cycles for MgTiO₃

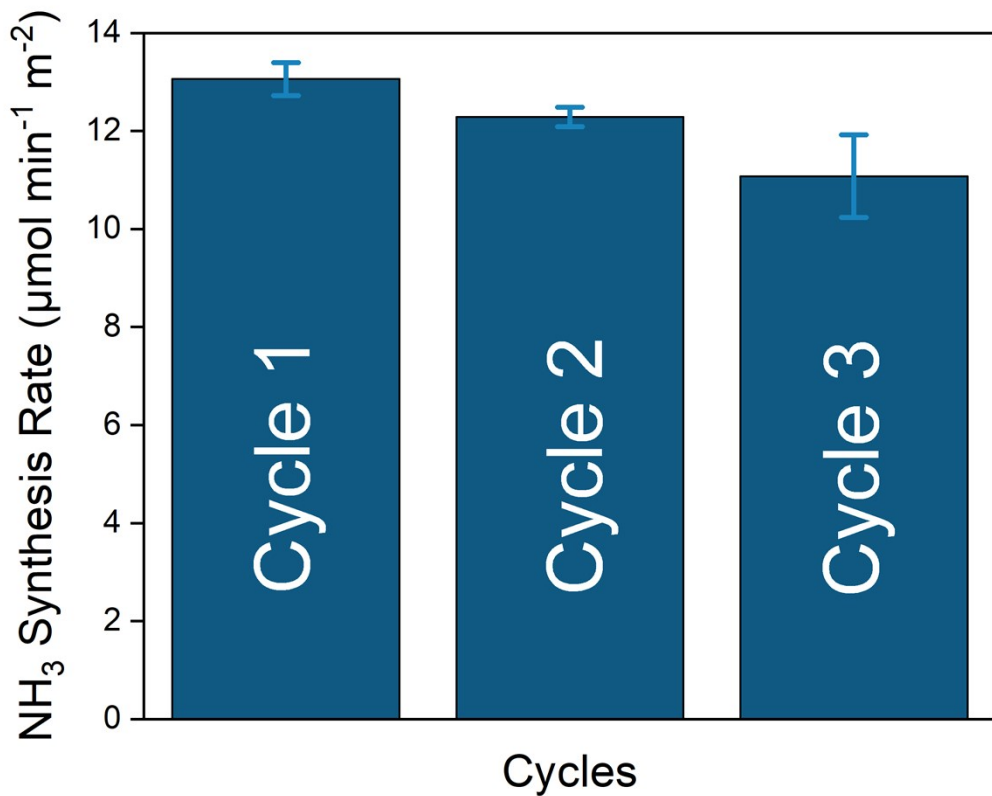


Figure S2 Assessment of catalytic activity after 6 reaction cycles for MgTiO_3 using an equimolar feed (1:1 $\text{N}_2:\text{H}_2$), every cycle consisting of 15 min.

Spent Perovskite (FTIR Spectra)

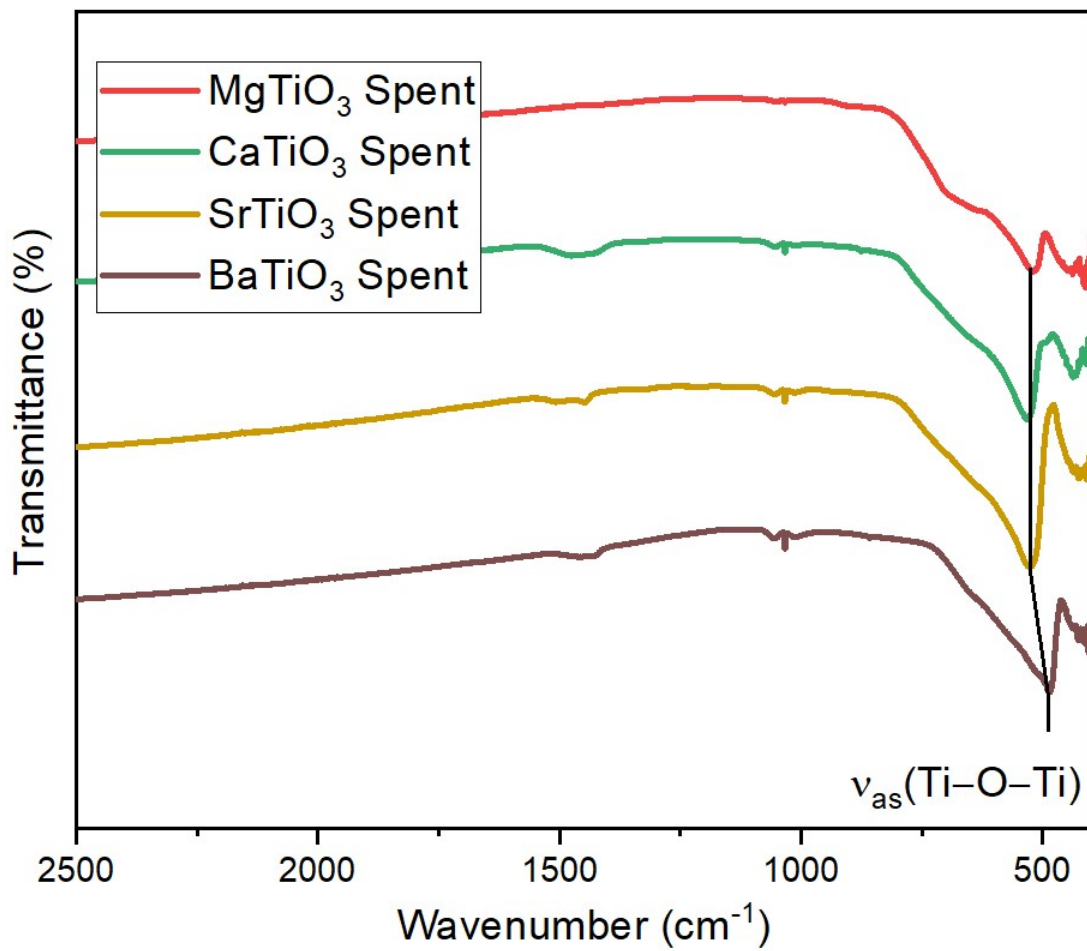


Figure S3. FTIR spectra of the spent perovskite samples.

OES for MgTiO₃ at different plasma Power (5W, 10W, 20 W)

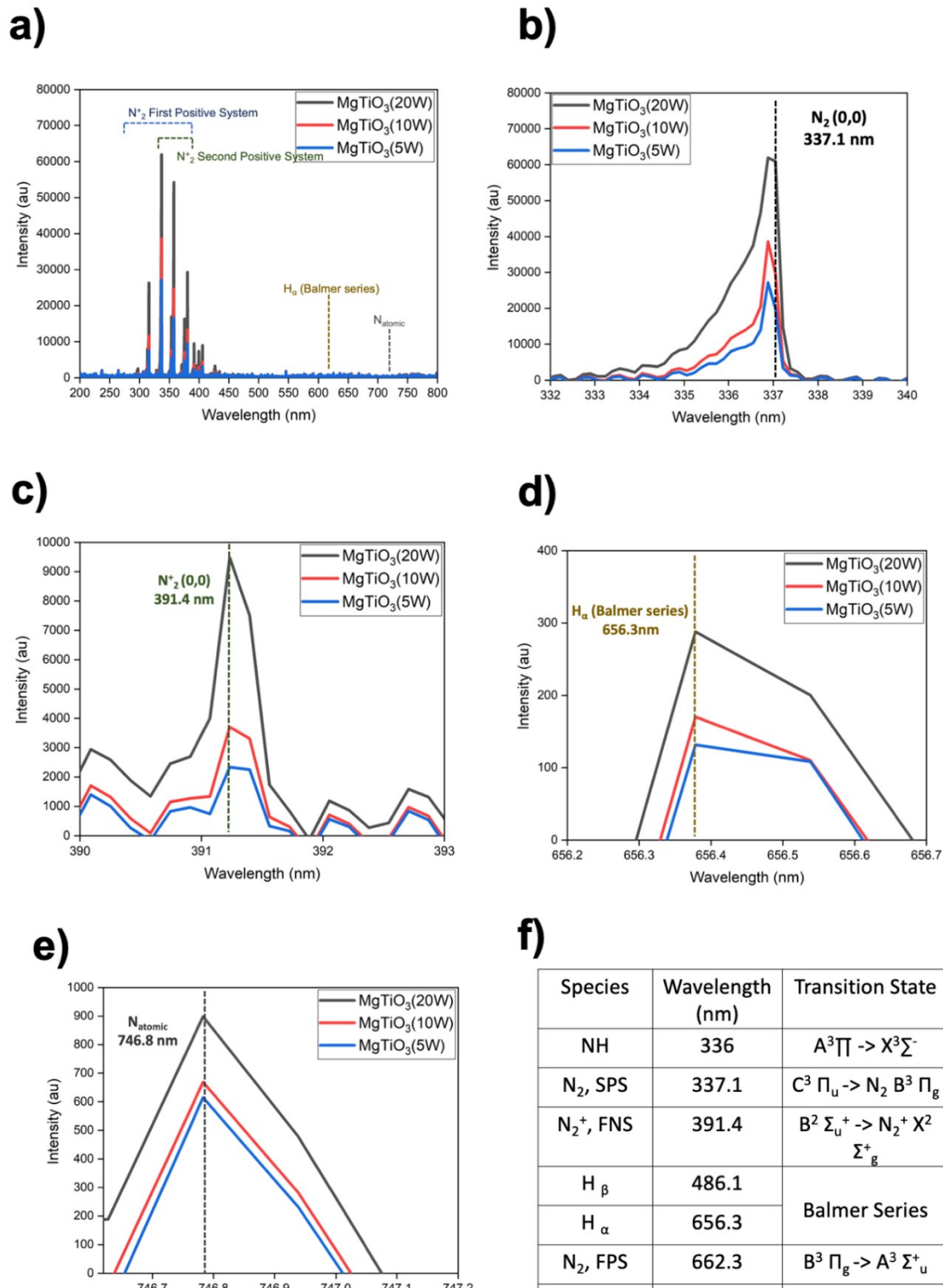


Figure S4 Emission spectra collected during plasma catalytic ammonia synthesis: (a), (b), (c), (d) Emission spectrum of N₂, N₂⁺, H_α, and N_{atomic} at 1:1 N₂:H₂ feed ratio MgTiO₃ at different Power (Watts) (5 W, 10 W, 20 W) (average bulk temperature of 155 °C) and f) summary of important plasma species.

Equations employed:

Equation S1:

NH_3 Synthesis rate =

$$\frac{GC \text{ area} * 0.745 \text{ (micromoles/sccm * s)}}{\text{Calibration factor}}$$

From Equation:

- NIST factor = 7.45E-7 mol/sccm * s-converting seconds to minutes = 60

- 1 mol= 1000000 micromoles

- $(7.45E-7 \text{ mol/sccm * s})(1000000 \text{ micromoles/1mol}) = 0.745 \text{ micromoles/sccm*s}$

$$\frac{\text{micromoles}}{\text{seconds}}$$

Units: $\frac{\text{micromoles}}{\text{seconds}}$

Note In order to calculate ($\mu\text{mol min}^{-1} \text{ g-catalyst}^{-1}$), divide ($\mu\text{mol min}^{-1}$) by grams of catalyst employed, In Presented study 0.1 grams of catalyst was loaded for each reaction in the plasma reactor.*

For further calculating synthesis rate per surface area ($\mu\text{mol min}^{-1} \text{ m}^{-2}$), divide the ($\mu\text{mol min}^{-1} \text{ g-catalyst}^{-1}$) by the BET surface area (m^2/g) for specific material employed.

Equation S2:

$$\frac{\text{Ammonia synthesis in (g/hr)}}{\text{Energy yield (g-NH}_3/\text{kWh)} = \frac{\text{Plasma Power (kW)}}$$

$$\frac{g/\text{hr}}{kW}$$

Units: $\frac{g/\text{hr}}{kW}$

Only Plasma ($\text{N}_2:\text{H}_2$) Vs Helium Dilution ($\text{N}_2:\text{H}_2:\text{He}$)

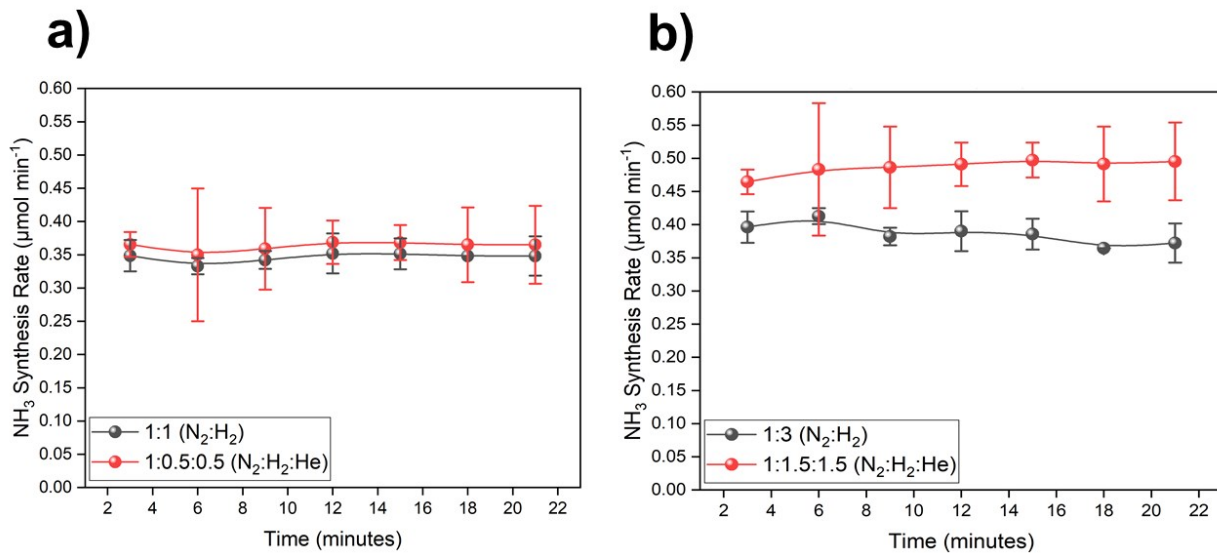


Figure S5 a) Ammonia synthesis rate for Plasma only Vs. Helium addition at two different feed ratio 1:1 ($\text{N}_2:\text{H}_2$) Vs. 1:0.5:0.5 ($\text{N}_2:\text{H}_2:\text{He}$) & 1:3 ($\text{N}_2:\text{H}_2$) Vs. 1:1.5:1.5 ($\text{N}_2:\text{H}_2:\text{He}$) flow ratio and total flow rate of 25 sccm at 5W.

OES for MgTiO₃ with & without Helium Dilution at Constant Watts.

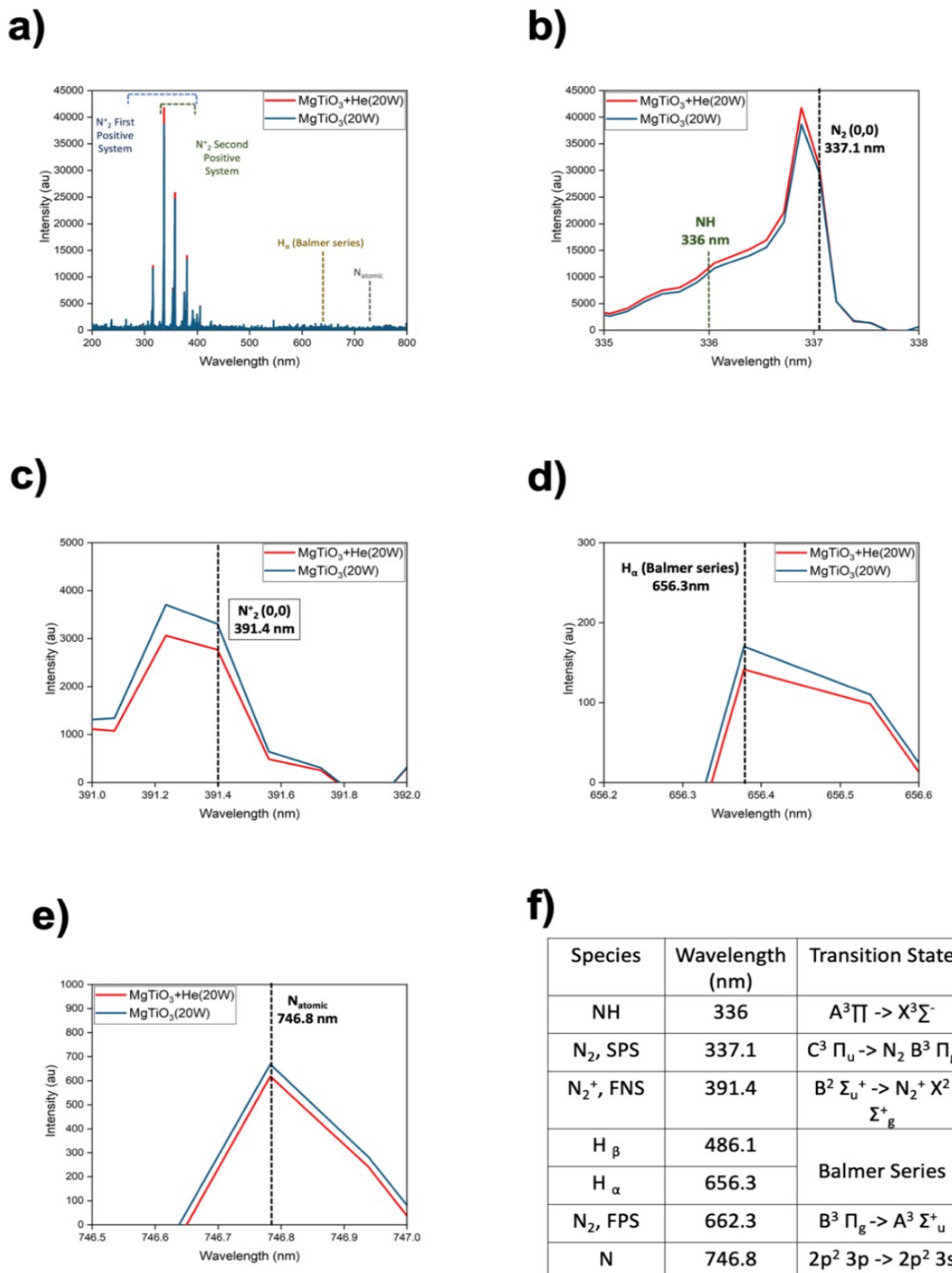


Figure S6 Emission spectra collected during plasma catalytic ammonia synthesis: (a), (b), (c), (d) Emission spectrum of N₂, NH, N₂⁺, H_α, and N_{atomic} at 1:1 N₂:H₂ feed ratio MgTiO₃ Vs 1:0.5:0.5 N₂:H₂:He feed ratio MgTiO₃ at different Power (Watts) (20 W) (average bulk temperature of 210 °C) and f) summary of important plasma species.

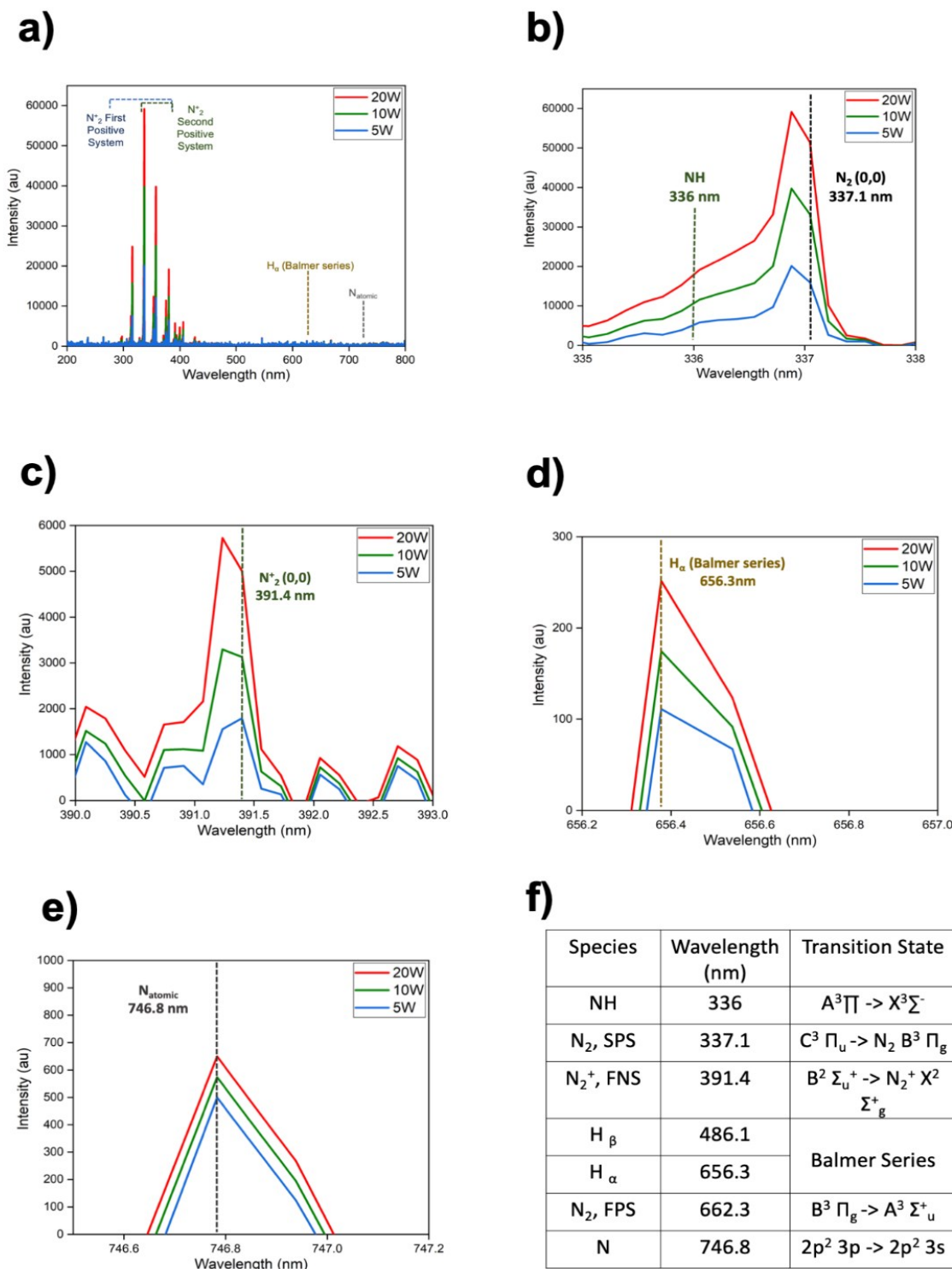


Figure S7 Emission spectra collected during plasma catalytic ammonia synthesis: (a), (b), (c), (d) Emission spectrum of N_2 , N_2^+ , H_α , and N_{atomic} at 1:1 $\text{N}_2:\text{NH}_3$ feed ratio MgTiO_3 at different Power (Watts) (5 W, 10 W, 20 W) (average bulk temperature of 163 °C) and f) summary of important plasma species.

OES for NH_3 Decomposition for MgTiO_3 at different Watts.

Comparison on perovskites performance (State-of-the-Art)

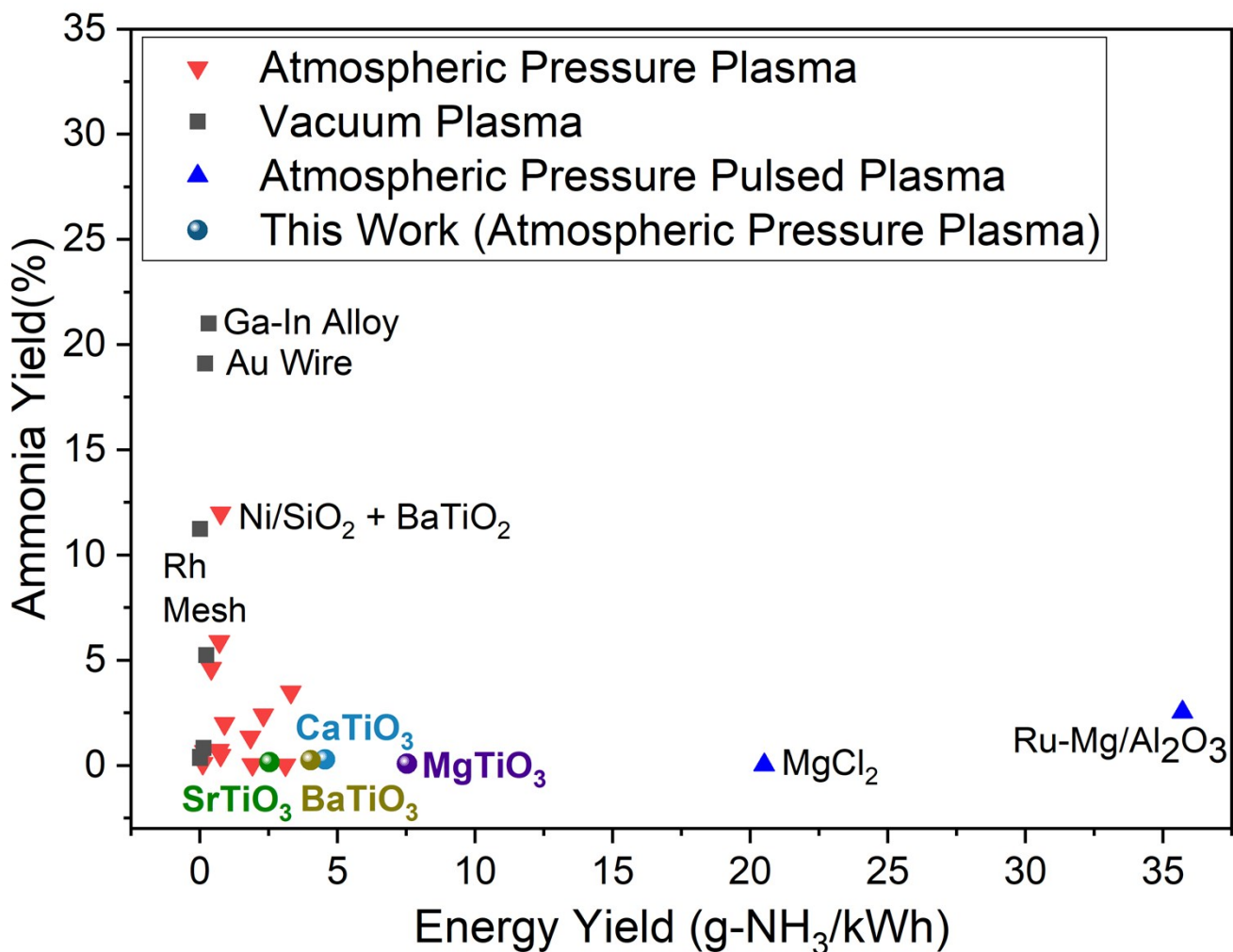


Figure S8 Comparison of perovskites performances of ammonia yield (%) versus energy yield (g-NH₃/ kWh) with highest values obtained by several research groups. Reproduced from ¹

Reactor Electrical Characterization

The electrical characterization was carried out by measuring the applied voltage to the reactor by employing a high voltage probe (Tektronix P6015A) and an oscilloscope (Tektronix TDS2014C). The reactor was operated at a frequency of approximately ~ 25 kHz. The complete electrical circuit can be found in our previous publication¹². The average power was calculated by finding the area under the curve for the V-Q Lissajous plot and multiplying it by the frequency. **Figure S1** shows the voltage-charge characteristics of the DBD reactor with MgTiO₃ as packing material. These measurements were performed under 1:1 N₂:H₂ feed ratio and 25 sccm total flow rate. The average measured powers for each material were collected 5 times.

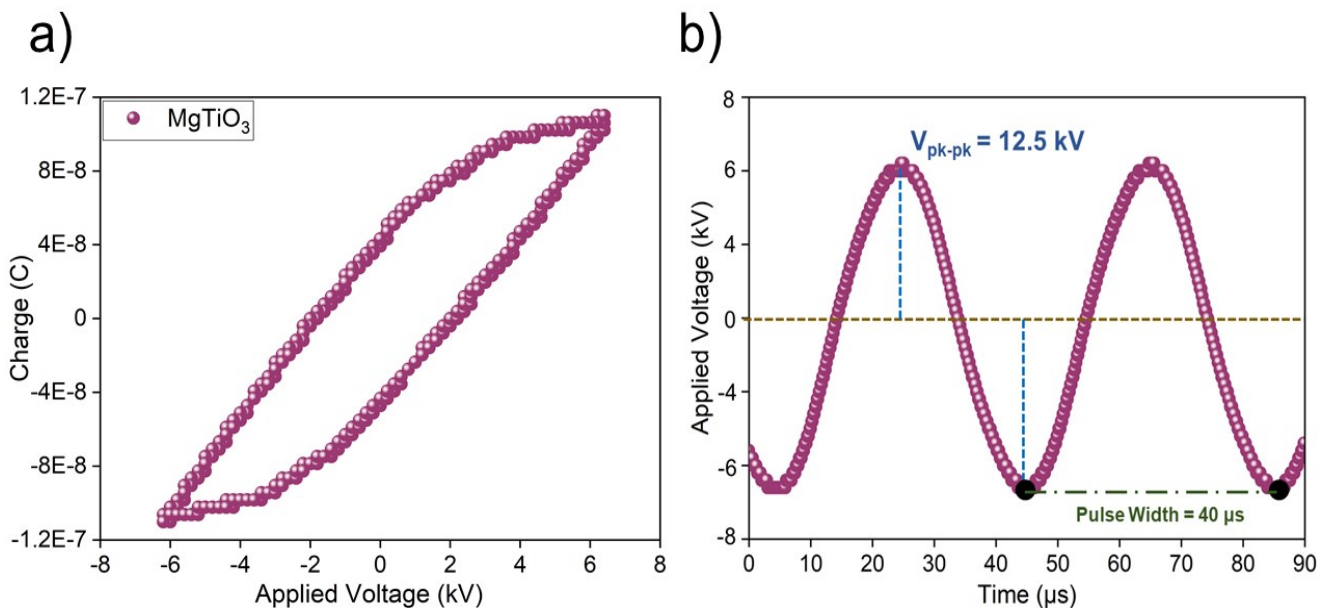


Figure S9 a) Applied voltage (kV) and charge (nC, across a capacitor) waveform collected using the oscilloscope for the N₂:H₂ ratio of 1:1. Lissajous curves generated using V-Q waveform for the studied MgTiO₃. b) Capacitor Voltage (V) Vs. Time (μs) at 10 watts for MgTiO₃.

Detailed data for Figure 8

Table S3 Summary of (Figure 8.) Dielectric Constant (ϵ_r) Vs. Energy Yield ($g-NH_3/kWh$)

Catalyst	Energy Yield $g-NH_3/kWh$	Standard Deviation	Dielectric Constant Value ϵ_r	Dielectric Constant References
-		±		-
ZIF-67	<i>1.19</i>	<i>0.09</i>	<i>2.3</i>	¹³
ZIF-8	<i>1.01</i>	<i>0.07</i>	<i>2.2</i>	¹³
SAPO-34	<i>1.29</i>	<i>0.04</i>	<i>2.6</i>	¹⁴
Fumed-SiO₂	<i>1.39</i>	<i>0.06</i>	<i>3.1</i>	¹⁵
MgO	<i>2.12</i>	<i>0.15</i>	<i>9.7</i>	¹⁵
MgTiO₃	<i>2.78</i>	<i>0.10</i>	<i>15</i>	^{16, 17}
CaTiO₃	<i>2.08</i>	<i>0.05</i>	<i>168</i>	¹⁸
SrTiO₃	<i>1.83</i>	<i>0.10</i>	<i>305</i>	¹⁸
BaTiO₃	<i>2.02</i>	<i>0.16</i>	<i>500</i>	¹⁹

Ammonia Calibration Curve

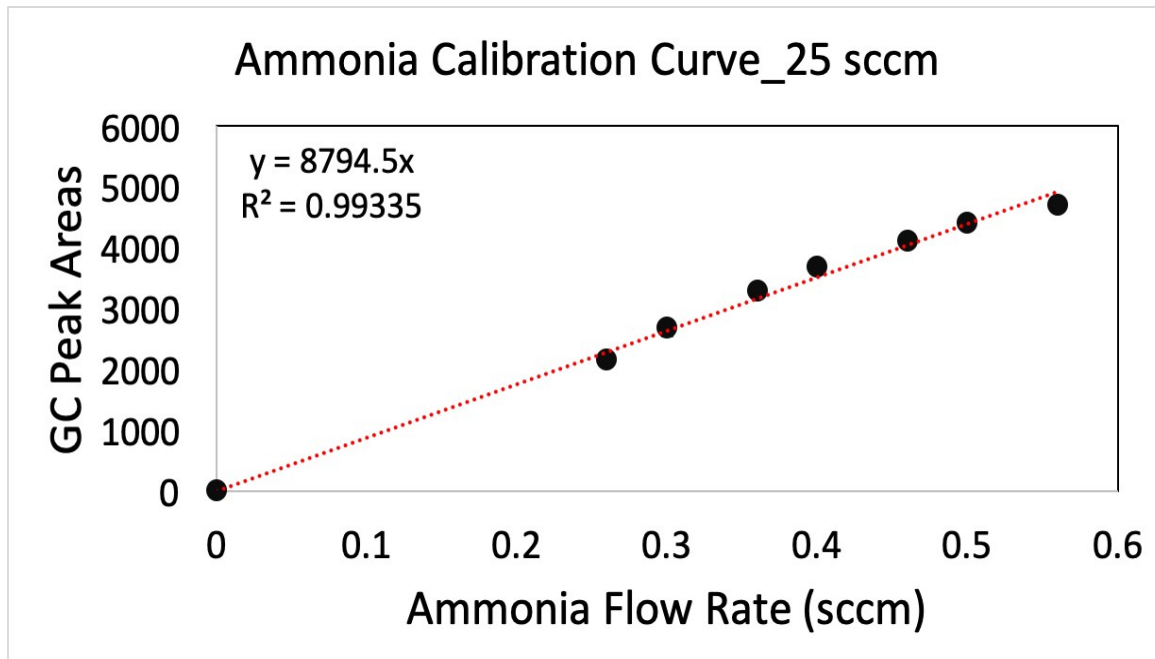


Figure S10 Ammonia Calibration curve.

Table S4 Ammonia Calibration curve details.

Ammonia sccm (X)	Area (Y)	Standard Deviation (Y error)	Standard Deviation (%)
0.00	0.00	0.00	0.00
0.26	2160.42	46.09	2.13
0.30	2680.41	132.30	4.94
0.36	3287.96	29.85	0.91
0.40	3676.92	26.77	0.73
0.46	4113.33	54.32	1.32
0.50	4400.76	13.38	0.30
0.56	4709.93	9.04	0.19

Live Gas Chromatography report for identification of ammonia peak

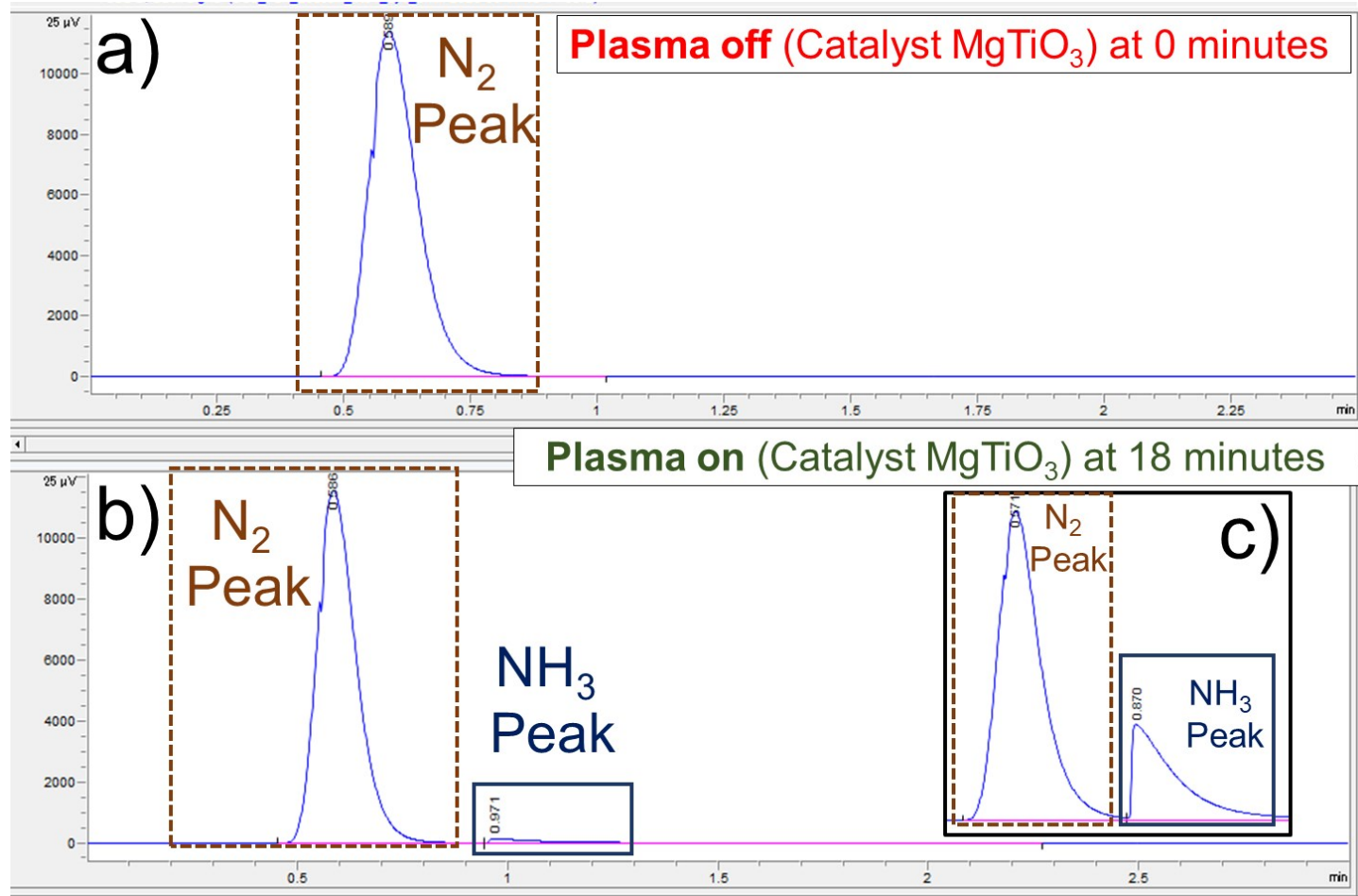


Figure S11 Quantification of Ammonia via Gas chromatography for MgTiO_3 catalyst a) Live GC report when there is no Plasma discharge at 0 minutes, indicating Nitrogen peak b) During Plasma catalytic reaction (at 18 minutes) indicating two peaks, Nitrogen followed by ammonia, c) Inset: Nitrogen + Ammonia calibration gas.

DBD Reactor Setup

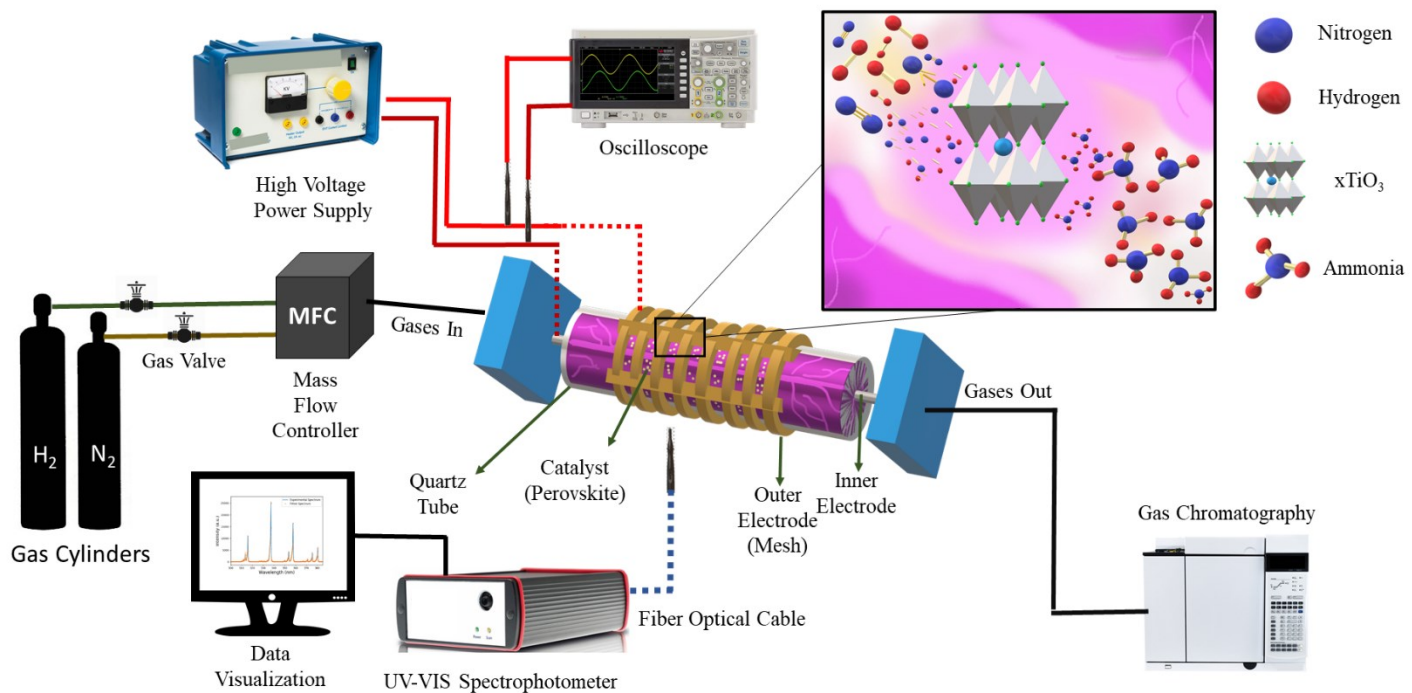


Figure S12 Schematic of Dielectric Barrier Discharge (DBD) reactor.

Catalyst Characterization (Surface Area)

Table S5 Surface area ($\text{m}^2 \text{ g}^{-1}$) of the perovskite samples.

Perovskite	Fresh ($\text{m}^2 \text{ g}^{-1}$)	Spent ($\text{m}^2 \text{ g}^{-1}$)
MgTiO₃	3.35	3.15
CaTiO₃	5.58	5.05
SrTiO₃	2.61	2.60
BaTiO₃	3.18	3.13

Perovskites Porosity (ϕ) (Fresh Vs. Spent)

Table S6 Textural properties of fresh perovskite catalysts.			
Perovskite	Surface area ^[a] (m ² g ⁻¹)	Total Pore Volume ^[b] (cm/g ⁻¹)	Porosity ^[c] (ϕ)
MgTiO ₃	3.35	0.002	0.006
CaTiO ₃	5.58	0.004	0.014
SrTiO ₃	2.61	0.002	0.008
BaTiO ₃	3.18	0.001	0.007

[1] BET method, [2] Measured at P/P₀ = 0.50, [3] **Equation S3**

Table S7 Textural properties of spent perovskite catalysts.			
Perovskite	Surface area ^[a] (m ² g ⁻¹)	Total Pore Volume ^[b] (cm/g ⁻¹)	Porosity ^[c] (ϕ)
MgTiO ₃	3.15	0.003	0.009
CaTiO ₃	5.05	0.003	0.012
SrTiO ₃	2.60	0.002	0.008
BaTiO ₃	3.13	0.002	0.012

[a] BET method, [b] Measured at P/P₀ = 0.50, [c] **Equation S3**

Porosity (ϕ) was calculated by dividing the total pore volume, measured from the N₂ isotherm at P/P₀ = 0.50, by the specific volume of the perovskite (**Equation S3**). The specific volume was taken as the inverse of the perovskite density: MgTiO₃, CaTiO₃, SrTiO₃, BaTiO₃ were 3.78, 3.98, 4.81, 6.02 cm³/g, respectively.

Equation S3

$$\phi = \frac{\text{Total Pore Volume } [\text{cm}^3/\text{g}]}{\text{Specific Volume } [\text{cm}^3/\text{g}]}$$

References

1. M. L. Carreon, *J. Phys. D*, **2019**, *52*, 483001.
2. K. Sugiyama, A. Kiyoshi, O. Masaaki, M. Hiroshi, M. Tsuneo and N. O.. *Plasma Chem . Plasma Process .* 1986, **6**, 179-193.
3. K.-i. Aika, T. Takano and S. Murata, *J. Catal.*, 1992, **136**, 126-140.
4. B. Mingdong, B. Xiyao, Z. Zhitao and B. Mindi, *Plasma Chem. Plasma Process.*, 2000, **20**, 511-520.
5. H. Bielawa, O. Hinrichsen, A. Birkner and M. Muhler, *Angew . Chem. Int.*, 2001, **40**, 1061-1063.
6. D. Szmigiel, H. Bielawa, M. Kurtz, O. Hinrichsen, M. Muhler, W. Raróg, S. Jodzis, Z. Kowalczyk, L. Znak and J. Zieliński, *J. Catal.*, 2002, **205**, 205-212.
7. P. Peng, Y. Cheng, R. Hatzenbeller, M. Addy, N. Zhou, C. Schiappacasse, D. Chen, Y. Zhang, E. Anderson and Y. Liu, *Int . J. Hydrot. Energy*, 2017, **42**, 19056-19066.
8. H. H. Kim, Y. Teramoto, A. Ogata, H. Takagi and T. Nanba, *Plasma Process Polym*, 2017, **14**, 1600157.
9. P. Peng, Y. Li, Y. Cheng, S. Deng, P. Chen and R. Ruan, *Plasma Chem. Plasma Process.*, 2016, **36**, 1201-1210.
10. B. S. Patil, A. S. R. Van Kaathoven, F. J. J. Peeters, N. Cherkasov, J. Lang, Q. Wang and V. Hessel, *J. Phys. D*, 2020, **53**, 144003.
11. H. Ronduda, M. Zybert, W. Patkowski, A. Tarka, A. Ostrowski and W. Raróg-Pilecka, *J Taiwan Inst Chem Eng*, 2020, **114**, 241-248.
12. J. R. Shah, F. Gorky, J. Lucero, M. A. Carreon and M. L. Carreon, *Ind. Eng. Chem . Res.*, 2020, **59**, 5167-5176.
13. M. Krishtab, I. Stassen, T. Stassin, A. J. Cruz, O. O. Okudur, S. Armini, C. Wilson, S. De Gendt and R. Ameloot, *Nat. Commun.*, 2019, **10**, 1-9.
14. M. Rybicki and J. Sauer, *Catal . Today*, 2019, **323**, 86-93.
15. J. Robertson, *EPJ Appl. Phys.*, 2004, **28**, 265-291.
16. B. D. Lee, H. Y. Ki, S. K. Eung and H. K. Tae, *Jpn J Appl Phys*, 2003, **42**, 6158.
17. V. M. Ferreira and J. L. Baptista, *Mater. Res. Bull.*, 1994, **29**, 1017-1023.
18. V. V. Lemanov, A. V. Sotnikov, E. P. Smirnova, M. Weihnacht and R. Kunze, *Solid State Communications*, 1999, **110**, 611-614.
19. B. H. Hoerman, G. M. Ford, L. D. Kaufmann and B. W. Wessels, *Applied physics letters*, 1998, **73**, 2248-2250.